RESEARCH ARTICLE

Histological study on maturation, fertilization and the state of gonadal region following spawning in the model sea anemone, *Nematostella vectensis*

Elizabeth Moiseeva, Claudette Rabinowitz, Guy Paz, Baruch Rinkevich*

Israel Oceanography and Limnological Research, National Institute of Oceanography, Tel-Shikmona, Haifa, Israel

* buki@ocean.org.il

Abstract

The starlet sea-anemone *Nematostella vectensis* has emerged as a model organism in developmental biology. Still, our understanding of various biological features, including reproductive biology of this model species are in its infancy. Consequently, through histological sections, we study here key stages of the oogenesis (oocyte maturation/fertilization), as the state of the gonad region immediately after natural spawning. Germ cells develop in a secluded mesenterial gastrodermal zone, where the developing oocytes are surrounded by mucoid glandular cells and trophocytes (accessory cells). During vitellogenesis, the germinal vesicle in oocytes migrates towards the animal pole and the large polarized oocytes begin to mature, characterized by karyosphere formation. Then, the karyosphere breaks down, the chromosomes form the metaphase plate I and the eggs are extruded from the animal enclosed in a sticky, jelly-like mucoid mass, along with numerous nematosomes. Fertilization occurs externally at metaphase II via swimming sperm extruded by males during natural spawning. The polar bodies are ejected from the eggs and are situated within a narrow space between the egg's vitelline membrane and the adjacent edge of the jelly coat. The cortical reaction occurs only at the polar bodies' ejection site. Several spermatozoa can penetrate the same egg. Fertilization is accompanied by a strong ooplasmatic segregation. Immediately after spawning, the gonad region holds many previtellogenic and vitellogenic oocytes, though no oocytes with karyosphere. Above are the first histological descriptions for egg maturation, meiotic chromosome's status at fertilization, fertilization and the gonadal region's state following spawning, also documenting for the first time the ejection of the polar body.

Introduction

Nematostella vectensis Stephenson, 1935 (Actinaria, Edwardsiidae), is a small widespread burrowing sea anemone living in estuaries along the Atlantic and Pacific coasts of North America

and the southeastern coast of England [1–3]). With a sequenced genome, *N. vectensis* has emerged as a model organism in developmental biology and metazoan evolution [4–9], as well as in ecological and toxicological studies [10–12].

Studies on *N. vectensis* in the last decade have focused on the origin of bilateral symmetry [13,14], the evolution of the mesoderm [15–17], the signaling pathways and the mechanisms of regeneration [18–27] the development of the nervous system [25], pattern formation [27] and more. However, our understanding of various biological features, including reproductive biology characteristics of this powerful model species are in its infancy.

N. vectensis, a gonochoristic species, spawns routinely under laboratory conditions [28]. Under different combinations of photoperiods, temperatures and diets it may spawn continuously throughout the year, forming mature eggs every 7–8 days [29]. Oocytes, which develop and mature in the mesenteries, are extruded through the mouth while immersed in a jelly coat as a part of the egg masses [5, 28, 29].

Primordial *N. vectensis* gametes were identified during embryogenesis and early development by exploring the expression of the *Vasa* and *Nanos* gene [30]. Histological data regarding developing oocytes and mature eggs [31, 32], including electron-microscopy descriptions [5, 33], have provided only slim information about oocyte growth and vitellogenesis. Attempts to determine the meiotic status of the chromosomes during egg ovulation and fertilization were unsuccessful [32, 34], and we are not familiar with studies that use histological descriptions of maturation and fertilization of the germ cells in *N. vectensis*. Lee et al. [35] documented two polar bodies during fertilization, but these observations were not illustrated in details. Thus, until now, the meiotic status of matured *N. vectensis* eggs during fertilization remains unclear, since no polar body ejection has been documented and the fertilization process was not shown histologically. Also, there is no detailed documentation of the morphological state of the gonadal region immediately following spawning.

This study thus aims to histologically investigate oocyte development during maturation and fertilization, as well as the structure and the composition of female sex cells in the gametogenic area of the mesentery immediately after spawning.

Materials and methods

Adult *Nematostella vectensis* individuals were cultivated according [36], with minor modifications according to [27, 28]. *N. vectensis* culture conditions are detailed in [37]. Males and females were reared in the same dishes (100x20 mm, cell culture dishes, cat. 664.160, Cellstar, Greiner bio-one, Germany) and gametes were taken as a result of natural spawning. Gravid females were fixed before spawning, at the onset and immediately after spawning. The animals were narcotized by adding 7.5% $MgCl_2$ to the culture dish and then fixed in Bouin's solution for 60–120 min or in 4% buffered formalin for 24 hours, at room temperature. Eggs were fixed at the moment of their extrusion from the female body as well as 3–5 minutes later in Bouin's solution for 15–30 min. After fixation, the samples were dehydrated in a graded ethanol series (70–100%), in a mixture of ethanol:butanol (I:I) and in 100% butanol and embedded in Paraplast (cat. P3683 Sigma Aldrich, St. Louis, MI, USA). Serial sections (4–5μm thick) were prepared using a rotary microtome (cat.2045, Jung Multicut, Leica). After staining, the sections were embedded in Entellan (Merck, Germany). Slides were observed under an Olympus BX50 upright microscope, equipped with a Color View camera (Soft Imaging System, Munster, Germany). A total of 7 adult females and 47 eggs from 3 egg masses were examined.

We used Mayer's alum hematoxylin and eosin (AHE) staining protocol to perform a standard histological examination, a periodic acid-Schiff's reagent (PAS-method) counterstained with alum hematoxylin (PAS-AH) for polysaccharides and an amylase treatment on parallel

sections as a control for glycogen; paraldehyde fuchsin—alcian blue (pH 2.8–3.0) (PAF-AB)–was used to identify mucins ('Steedman's method') [38], in combination with eosin or azocarmine G. For mucopolysaccharides we used alcian blue with the PAS-method and alum hematoxylin (AB-PAS-AH) [39]; for nuclear staining either DAPI or ethidium bromide (EtBr) were used.

Immunolabeling for phospho-histone H3 (ser 10-R; specificity checked in ref. 23) was performed using commercial rabbit polyclonal antibodies (Santa Cruz Biotechnology, USA). Blocking for nonspecific binding sites was performed with 1% bovine serum albumin dissolved in 50 mM TBS for 4 h incubations at room temperature. The blocking solution was replaced with commercial rabbit polyclonal-primary-antibodies (Santa Cruz biotechnology, USA) diluted in blocking buffer (1:400) for an overnight incubation, followed by a 2 h incubation with a goat anti-rabbit secondary antibody (1:400), conjugated to the fluorescence Cy3™-AffiniPure, Goat anti-Rabbit IgG Amax-550 and Emax-570 (Cat No. 111-165-003; Jackson ImmunoResearch Laboratories, Pennsylvania, USA).

All slides were mounted in a Fluoromount medium (cat F4680; Sigma, Germany) and photographed using the Olympus Bx50 upright fluorescent microscope.

Results

General morphology

The morphological features of *N. vectensis* individuals have been previously described [1,2,16,40]. General view of the adult animal is shown in Fig 1A. It is evident that this sea anemone has no true ovaries [5], whereas a "gonad" in *N. vectensis* is the determined gametogenic area of the mesentery, which is located between the retractor muscles and the mesenterial filaments (Fig 1B). This zone can be further differentiated from other mesenterial areas by its cytomorphological characteristics: it hosts the germ cells exclusively (Fig 2A), so in this article we use the term "gonadal region". The general morphology of the gonadal regions of the pre-spawning and post-spawning anemones do not differ, with the exception of the sex cells composition. In order not repeat description, we considered it expedient to simultaneously describe the general morphology for both pre-spawning and post-spawning individuals. The
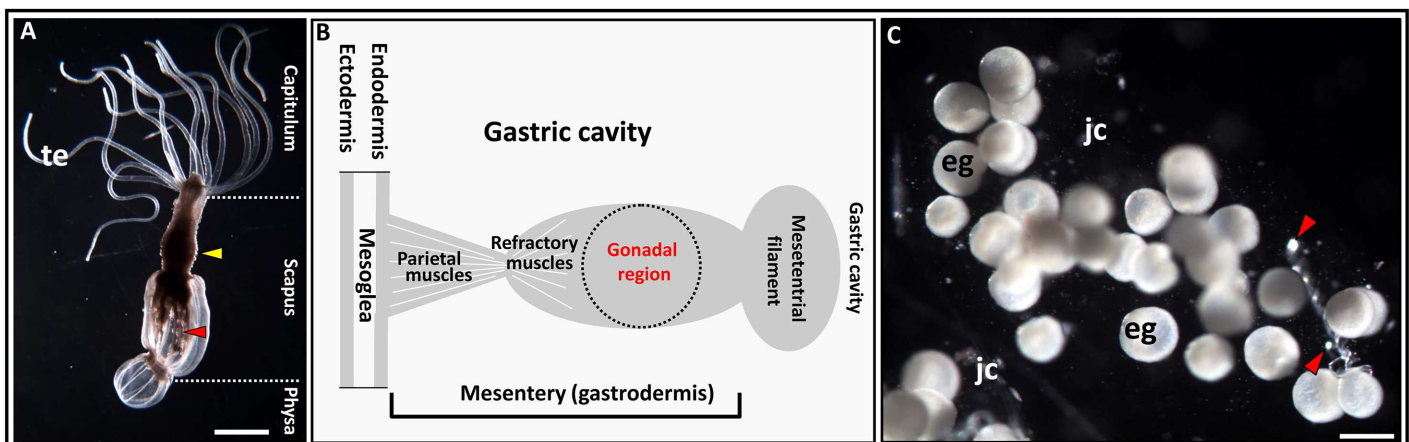
Fig 1. General view of the adult *Nematostella vectensis*. A. Three main body parts are shown. Yellow arrowhead indicates the location of the gonadal region within the body; red arrowhead indicates the mesentery within the scapus. **B**. A schematic drawing of the gonadal region localization within the mesentery in transverse section. **C**. The egg masses with eggs and the nematosomes (arrowheads). eg, egg; jc, jelly coat; te, tentacles. Scale bars: A = 2.0 mm, C = 200 μm.
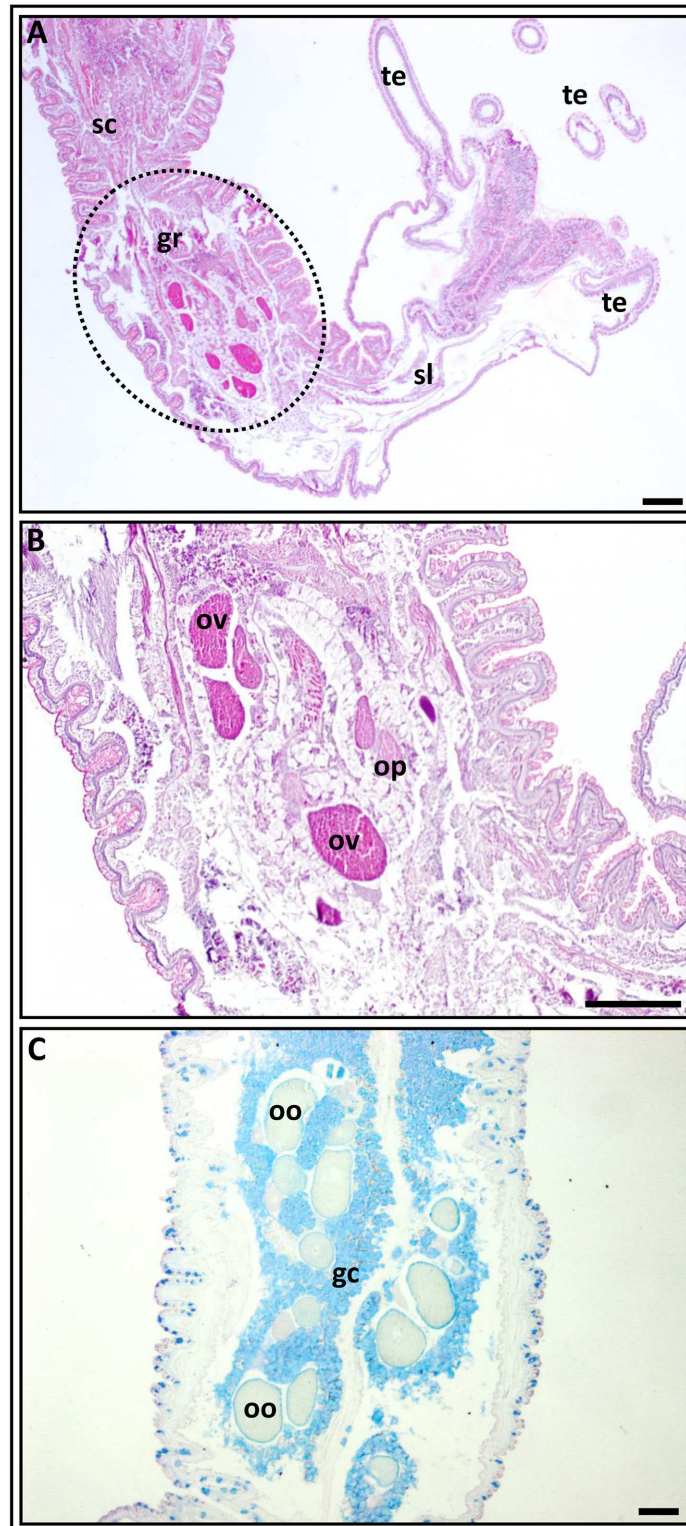
Fig 2. Longitudinal sections through a gravid *Nematostella*'s mesentery. A. The upper part with tentacles (te), the scapulus (sl) and part of the scapus (sc) with the gonadal region (gr) (outlined) are seen. **B.** A higher magnification of the outlined zone in "A" reveals germ-cells groups with vitellogenic (ov) and previtellogenic (op) oocytes, and glandular cells surrounding them. Vitellogenic oocytes are strongly stained with azocarmine. PAF-Az stain. **C.** The germ-cells groups in the gonadal region, which contain selectively

colored AB-positive glandular cells (gc) surrounding colorless oocytes (oo), can be seen. PAF-AB stain. gc, glandular cells; oo, colorless; oocyte; op, previtellogenic oocyte; ov, vitellogenic oocyte; sc, scapus; sl, scapulus; te, tentacles. Scale bars = 100 μm.

gonadal region consists of several local germ-cells groups (>10 groups/middle cross section), (Figs 2B, 2C, 3A and 3B). Inside one group oocytes are developed asynchronously, so all stages of oogenesis are represented from small previtellogenic oocytes to large vitellogenic and maturing ones (Figs 2B, 3A, 3B, 4 and 5). In addition to oocytes of different stages of development, the gonadal region possesses the vacuolated gastrodermal cells (glandular elements), forming a loose network around germ cells (Figs 2C and 3B–3E), as well as the trophocytes (accessory cells) (Fig 3D–3F). Glandular cells are stained by alcian blue (Figs 2C, 3D, 3F and 4B and positively stained by Schiff-reagent (Figs 3E and 4C), thus revealing the existence of various polysaccharides, mucopolysaccharides and mucoproteins. When using the AB-PAS stain, the vacuolar membrane and the filaments within the vacuoles are stained light green and pink, respectively (Fig 4B and 4C). AHE reveals that the vacuole's content does not stain with hematoxylin, and so it appears to be a light pinkish hue (Fig 3C). Furthermore, the glandular cells' PAS-positive material retains its color after the 1% amylase treatment (30 min, room temperature), indicating it is not a glycogen. Trophocytes, which are groups of dense, small cells, are situated between the glandular cells. During growth and development of oocytes, they are formed in the trophonema which is a unique association of germ and somatic cells [5]. The trophonema is clearly visible in large polarized previtellogenic and vitellogenic oocytes and is distinct in oocytes remaining in the gonad region after spawning. In the trophonema location the invagination of outer ooplasmatic layer can be seen (Figs 3C, 3E and 4A).

Maturation

At the end vitellogenesis the large polarized oocytes reach a diameter 130–160 μm, germinal vesicles are 50–70 μm. Germinal vesicles are located in the region of the animal pole. The karyoplasm can be strongly stained by eosin; yolk inclusions are evenly distributed throughout the ooplasm (Fig 4E). They are intensively stained by eosin and show a strong PAS-reaction (Fig 4C and 4E) that remains following the treatment with amylase. The cortical layer of ooplasm is well defined (Figs 3C, 3E, 3F and 4C) and its external edge is visible "rough" (Fig 4E)

The oocyte's transition into maturation process is characterized by the formation of the karyosphere at the animal pole of the cell (Fig 5). The karyosphere is a modified germinal vesicle. During the formation of the karyosphere a gradual condensation of chromosomes occurs. The germinal vesicle loses its normal morphology and is transformed into an amorphous structure, the location of which is distinctly separate from other zones of oocyte (Fig 5A). The karyosphere's form is variable, and most often it is composed of three parts: a relatively homogeneous light substance, a denser, lumpy substance and a ring zone (Fig 5B and 5C). The chromosomes, which can be located at any part of the karyosphere, are very condensed. They form crystalline lumps and display the same weak PAS-reaction as the yolk granules. DAPI and EtBr staining are usually observed in the dense crystalloid formation (Fig 5C and 5D). Yolk inclusions are evenly located in the ooplasm, with no visible gradient in distribution between the animal and the vegetative poles (Fig 5A). The cortical layer stains strongly and its external layer appears rough (Fig 5A), like in the large vitellogenic oocyte (Fig 4E). The cortex's granules are marked by a darker color, which strongly differs from the color of the glandular cells that surround the germ cells (Fig 5A and 5B).
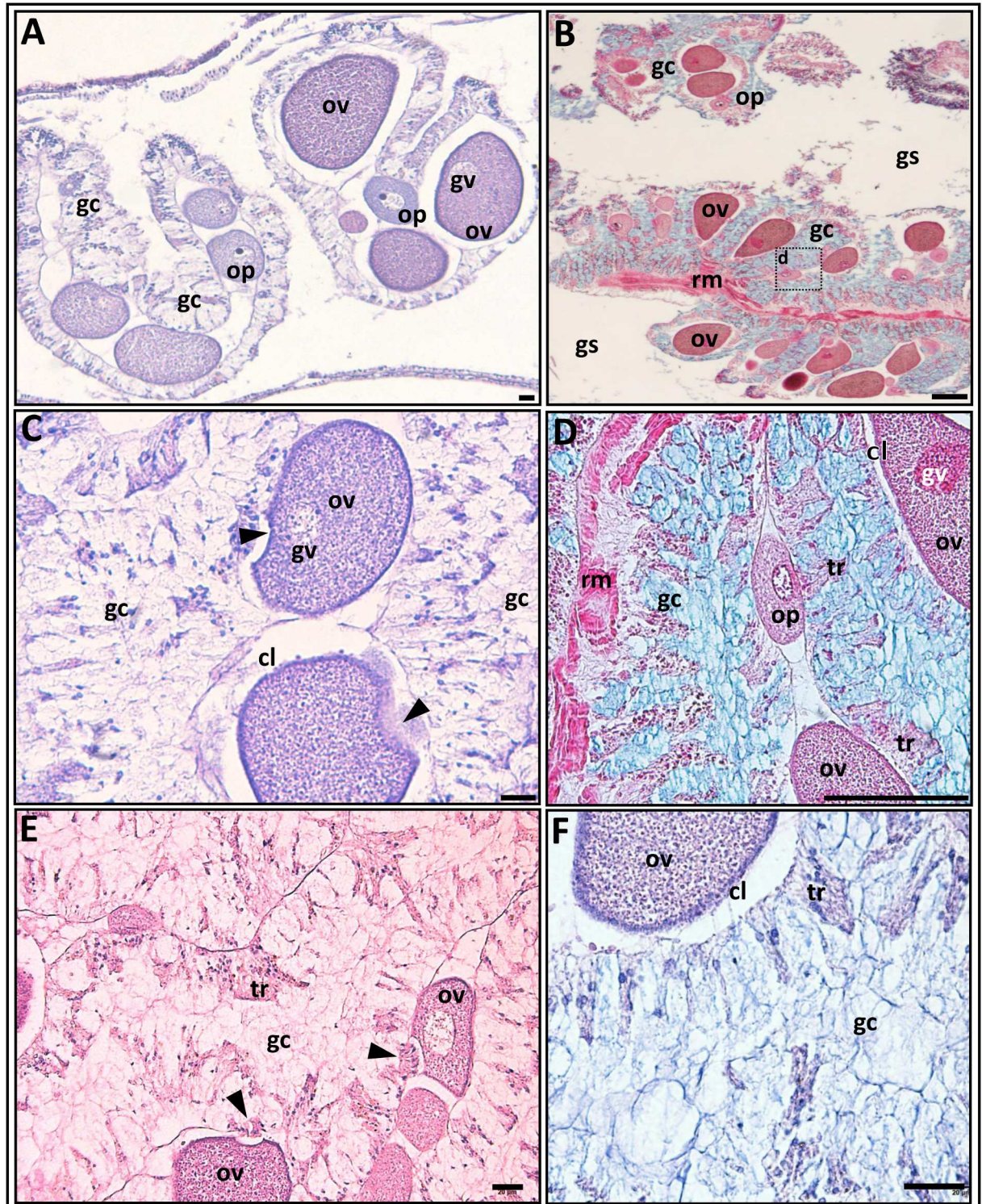
Fig 3. The gonadal region immediately after the extrusion of an egg mass. A. A general view of the gonadal region in a cross section. Germ-cells groups are well visible. AHE stain; **B**. The longitudinal section of the gonadal region part. The gastric cavity (gs) is empty and clearly visible. Groups of germ cells at different stages of oogenesis and the glandular cells (gc) that surround them are seen within the gonadal region. PAF-AB-Az stain. **C**. Vitellogenic oocytes (ov) with an invagination of the oolemma (arrowhead). AHE stain. **D.** The part of the gonadal region seen in '**B**' at a higher magnification. Note the bands of trophocytes (tr) between the glandular cells. PAF-AB-Az stain. **E,F.** Glandular cells show a reduced intensity of staining with reagent Schiff (PAS-AH stain in **E**) and alcian

blue (AB-AHE stain in **F**) as compared to pre-spawning stage (Fig 4B and 4C; in both dyes, the fixation and staining periods were identical). In '**E**' the vitellogenic oocytes with an invagination of the oolemma and trophonema (arrowheads) are seen. cl, cortical layer; gc, glandular cells; gs, gastric cavity; gv, germinal vesicle; op, previtellogenic oocyte; ov, vitellogenic oocyte; rm = retractor muscle; tr, trophocytes. Arrowheads in **C** show invagination of the oolemma; arrowheads in **E** show trophonema. Scale bars = 20 µm.

https://doi.org/10.1371/journal.pone.0182677.g003

By the end of the maturation process the chromosomes progress from stage of the prophase meiosis I to the metaphase stage. The metaphase plate lies just below the surface of the oocyte, among the yolk globules, and is barely visible. Ovulation takes place in the gastrovascular cavity in concert with the formation of the protective jelly coat, and then the eggs together with the numerous nematosomes, containing nematocyst capsule, are extruded from maternal organism in the form egg mass (Fig 1B). The jelly coat is made from a variety of mucins all with tinctorial properties similar to the content of the gonadal region's glandular vacuolated cells (Fig 6B, 6G and 6H).

Fertilization

The diameters of the fertilized eggs range between 158 and 175µm. Fertilization occurs when the chromosomes are in the metaphase II stage (Fig 6A), concurrent to the emission of the first polar body, as revealed by the simultaneous presence of the polar body and the spermatozoa or male pronucleus (Fig 6C, 6D and 6H). The first polar body (about 25µ) is larger than the second body and contains a small amount of chromatin (Fig 6D–6F). The male pronucleus passes through the oolemma and moves in the direction of the female pronucleus. As the nuclear membrane of the fertilizing spermatozoa dissolves, the male pronucleus is revealed as an amorphous, borderless, finely-granular structure (Fig 6C–6F). The female pronucleus looks like a light bubble with condensed chromosomes inside (Fig 6C, 6D and 6L). We have documented cases where several spermatozoa penetrated the egg, they can be seen as dark spots (with dissolved head membranes) inside the ooplasm (Fig 6L). During fertilization the adjacent internal layer of the jelly coat is separated from the oolemma exactly at the animal pole's location, allowing the polar body to be shed (Fig 6B). The perivitelline space appears only at the animal pole, suggesting that the cortical reaction takes place precisely in this zone. The outermost edge of the oolemma at the fertilized egg's animal pole looks very uneven and rough (Fig 6L and 6K), while the edge of the same egg's vegetative pole has a smooth outline (Fig 6L). The spermatozoa's penetration into the egg is accompanied by ooplasmic segregation, during which fine and small yolk inclusions move and concentrate into the egg's central zone while large granules and globules of yolk remain at its periphery. As a result, the central zones appear more densely stained than the peripheral zones (Fig 6C, 6F, 6E and 6G). The ooplasmic segregation is crucial for following the spatial organization of the embryo tissues [38].

The morphology of the gonadal region immediately after spawning

After the egg mass has left the female body, left over germ-cells groups within the gonadal region become clearly visible (Fig 3A and 3D), containing in each group previtellogenic and vitellogenic oocytes of different sizes that are also surrounded by gastrodermal glandular cells (Fig 3B–3E). The larger polarized previtellogenic oocytes are marked by an invagination of the oolemma, which occurs at the same location as the trophonema (Figs 3C, 3E and 4A). The nearly colorless nucleoplasm contains rough chromosome threads (lampbrush chromosomes) and 1–2 large eccentric nucleoli (Fig 4A). In some oocytes H3 phosphorylation is well expressed suggesting that the chromosomes are in prophase I meiosis (Fig 4D). The vitellogenic oocytes of different sizes contain varied amounts of yolk inclusions, which stain strongly with eosin and give PAS-reaction that persists after amylase treatment (Fig 3C and 3E). In all
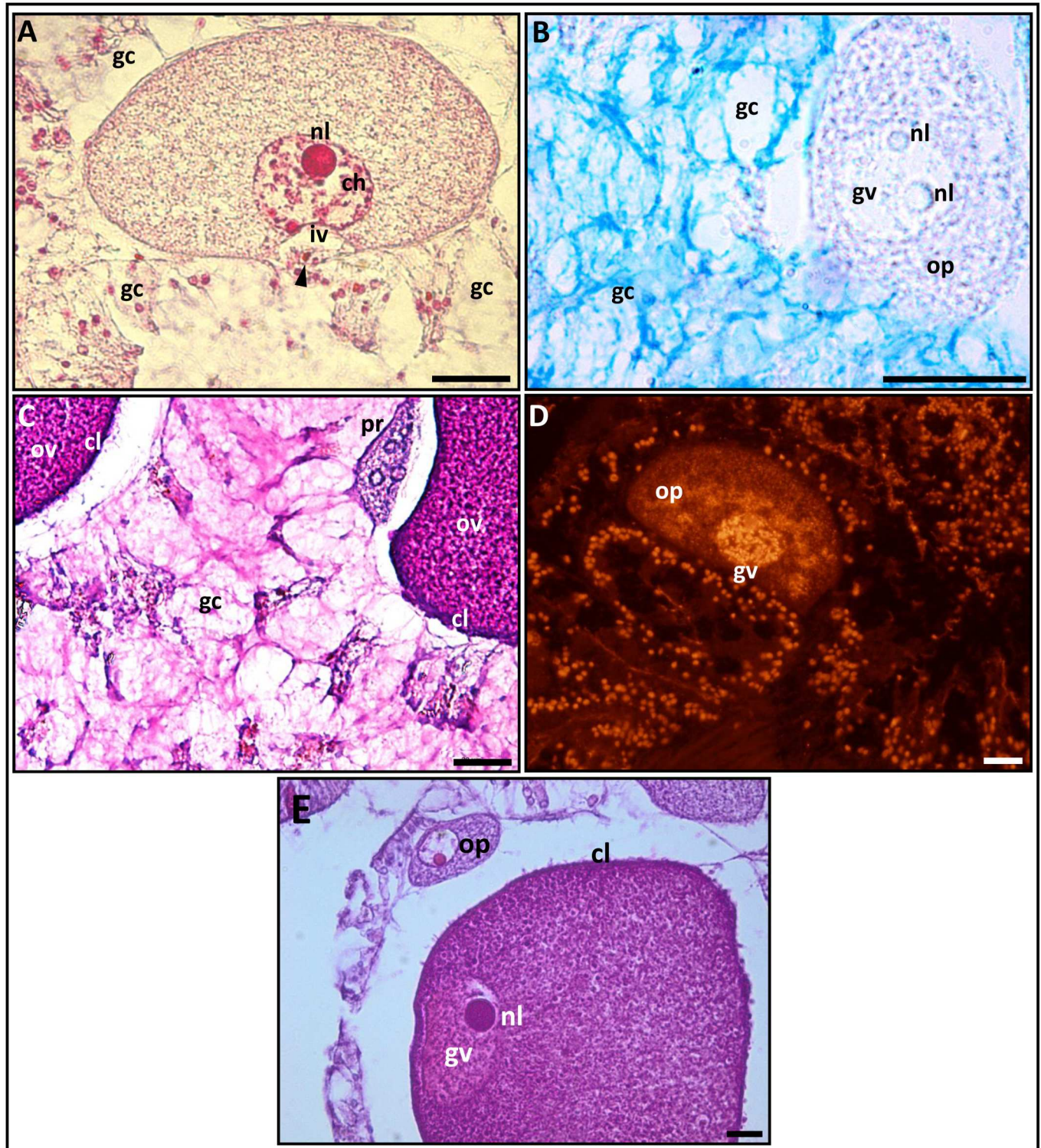
Fig 4. Oocytes of the different stages of oogenesis and the glandular cells surrounding the oocytes within the germ-cells groups. A. The polarized previtellogenic oocyte, characterized by lamp-brush chromosomes (ch) inside the germinal vesicle, the oolemma's invagination (iv) and the trophonema (arrowhead), which is well developed in the site of invagination. PAF-Az stain. **B,C.** Alcian blue-positive (**B**) and PAS-positive (**C**) glandular vacuolated cells (gc). The previtellogenic oocyte (op) (colorness in 'B') with nucleoli (nl) inside germinal vesicle (gv) and the vitellogenic oocytes (ov) are filled of the yolk granules (in '**C**') can be seen. PAF-AB and PAS-AH stain, respectively. **D.** Histone H3 phosphorylation in prophase I meiosis chromatosomes in the germinal vesicle of a previtellogenic oocyte. **E.** The oocyte of the end of vitellogenesis. The germinal vesicle is located

at the animal pole under the cortical layer (cl) of the ooplasm, and the ooplasm is filled with yolk granules and globules. The external edge of the cortical layer is visible"rough". ch, chromosomes; cl, cortical layer; gc, glandular cells; gv, germinal vesicle; iv, invagination of the oolemma; nl, nucleoli; op, previtellogenic oocyte; ov, vitellogenic oocyte. Arrowhead shows trophonema (in **A**) AHE stain. Scale bars: A-D = 20 μm, E = 10 μm.

cases observed the largest remaining vitellogenic oocytes in the gonadal zone do not yet contain the karyosphere, although the invagination of oolemma in the animal pole is noticeable, the cortical layer is well defined and the germinal vesicles are located near this invagination (Fig 3C and 3E). The abundance of glandular cells does not vary noticeably, but the staining of the cells is less intensive, as a result of a certain amount of secretory substances that have
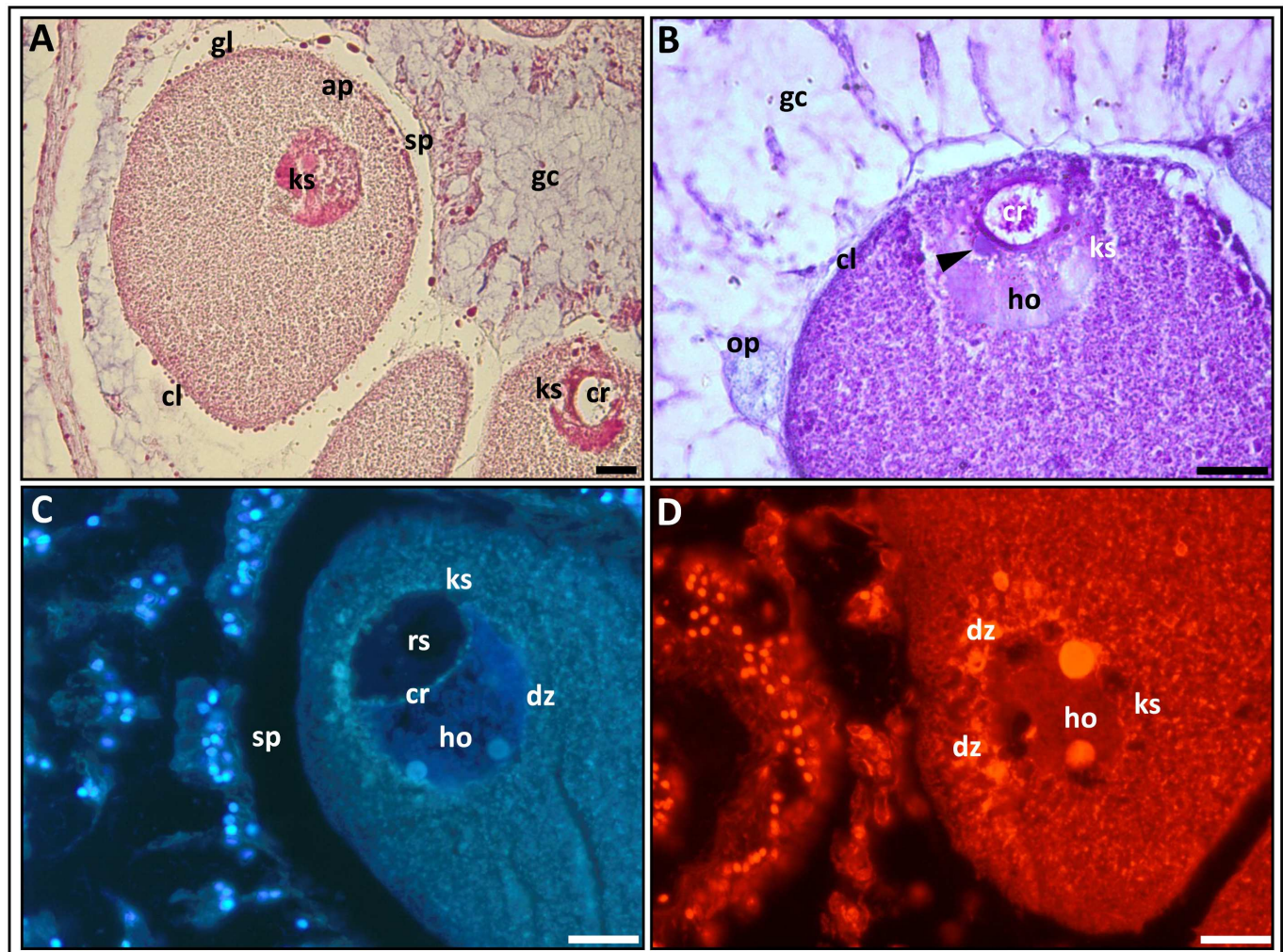

Fig 5. The karyosphere (ks) in maturing oocytes. A. A general view of an oocyte with karyosphere. The yolk globules (gl) along the edge of the cortical layer (cl) and the space (sp) between the oolemma and the gastrodermal cells are seen. PAF-Az stain. **B.** Three karyosphere zones are visible: a relatively homogenous substance (ho), a denser, lumpy substance (arrowhead) and a ring-shaped zone. The chromosomes (cr) are inside the ring-shaped zone. AB-PAS stain. **C.** Condensed chromosomes (cr) are in the dense zone of the karyosphere. Note the space (sp) between the oolemma and the gastrodermal cells. DAPI stain. **D**. Chromosomes are in dense zone of the caryosphere during condensation. EtBr stain. cl, cortical layer; cr, chromosomes; dz, dense zone; gc, glandular cells; gl, yolk globules; ho, gomogenous zone; ks, karyosphere; op, previtellogenic oocyte; rz, ring-shaped zone; sp, space between the oolemma and gastrodermal cells. Arrowhead shows the dense zone of the karyosphere (in **B**). Scale bars = 20 μm.
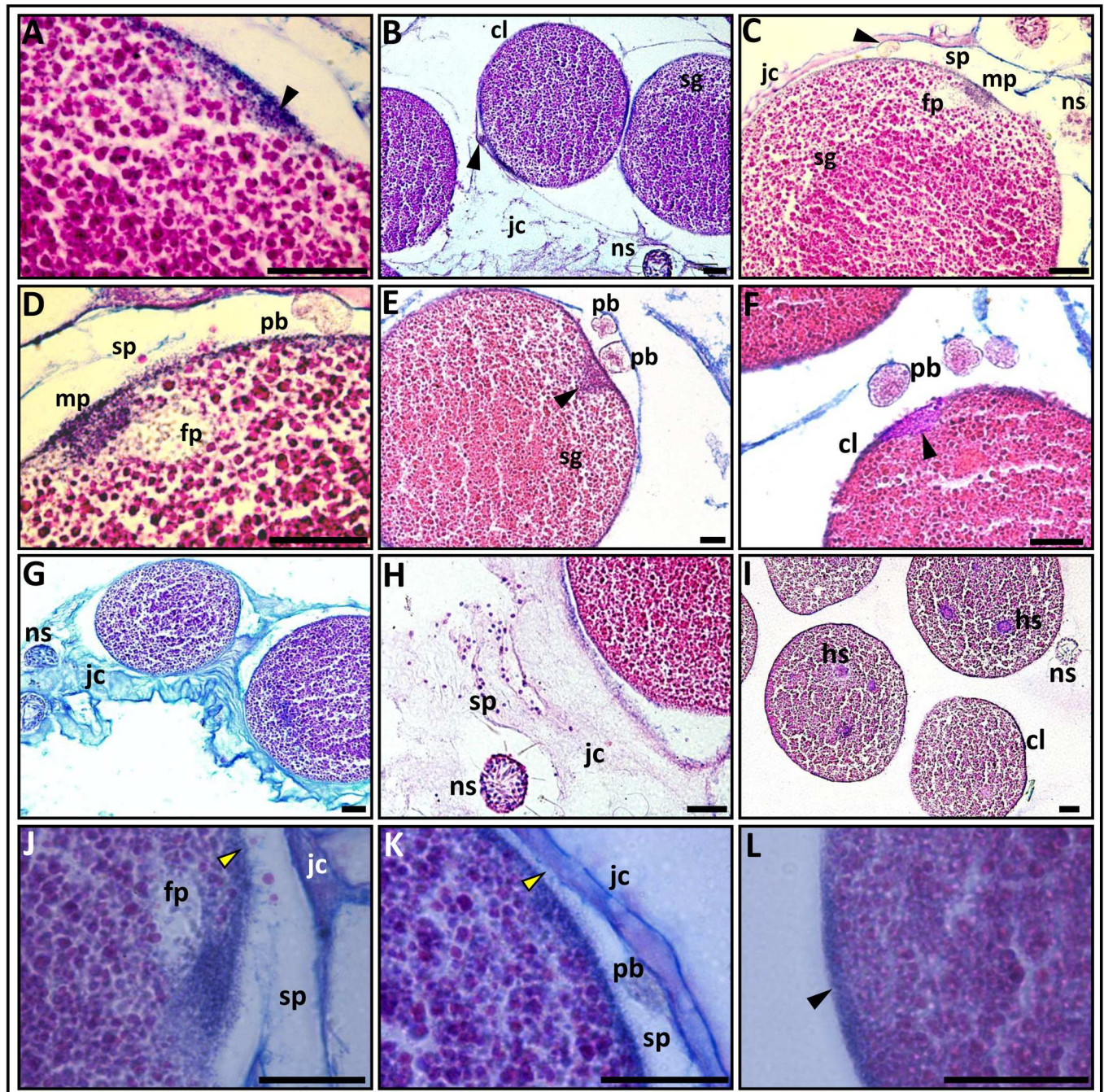
Fig 6. Mature eggs during fertilization. A. The metaphase II plate is located at the animal pole of the egg (arrowhead); AB-PAS-AH stain. **B.** The first polar body (arrowhead) that appeared in the space between the oolemma and edge of the jelly coat (jc). The segregated ooplasm (sg) is seen. AB-AHE stain. **C.** A general view of the animal pole during fertilization. The first polar body (arrowhead), the male pronucleus (mp), the female pronucleus (fp), the space (sp) between the oolemma and the edge of the jelly coat and the segregated ooplasm are seen. PAS-AB-AH stain. **D**. A higher magnification of the animal pole shown in '**C**'. The polar body (pb) is clearly seen in a state of division. **E,F.** The formation of two (**E**) and three polar bodies **(F)**. The male pronucleus (arrowhead) is located in the peripheral zone of the egg (the coarse-grained yolk area) and the segregated ooplasm (in '**E**') are clearly visible. AB-PAS-AH stain. **G**. Eggs located within the jelly coat. The ooplasmatic segregation is clearly visible. Inside the jelly coat are nematosomes (ns). AB-AHE stain. **H.** Numerous spermatozoa (sz) and one nematosome are seen inside the jelly coat. AHE stain. **I.** Some sperm heads (hs) are seen inside the eggs. They are visible as dark spots. AHE stain. **J.K.** The edge of the cortical layer (arrowheads) at the animal pole is characterized by a rough view. Fine granules are seen in the space between the oolemma and the internal edge of the jelly coat. In '**J**' the female pronucleus is clearly seen, in '**K**' the polar body is depicted. **L.** The edge of the cortical layer at the vegetative pole of the same egg is smooth (arrowhead). AB-AHE stain. cl, cortical layer; fp, female pronucleus; hs, sperm heads; jc, jelly coat; mp, male pronucleus; ns, nematosome;

pb, polar body; sg, segregated ooplasm; sp, space between the oolemma and the edge of the jelly coat; sz, spermatozoa. Arrowhead in **A** shows metaphase II plate; arrowheads in **B** and **C** show the polar bodies; arrowheads in **E** and **F** show male pronuclei; yellow arrowheads in **J** and **K** illustrate a rough view of the cortical layer edge at animal pole and arrowhead in **L** shows a smooth view of the cortical layer at the vegetative pole in the same egg. Scale bars = 20 μm.

already been released together with the eggs (Fig 3E and 3F). The trophocytes appear as longitudinal strands located between groups of glandular cells (Fig 3D–3F)

Discussion

In this study key stages of the oogenesis (maturation and fertilization) of *Nematostella vectensis* and the state of the gametogenic region at the mesentery immediately after spawning are studied using light microscopy with different staining approaches. These stages of oogenesis are described for the first time, as are the identification of the chromosomal status at the moment of fertilization and the documentation of the polar bodies. These findings supplement the information currently available regarding the reproductive biology of *N. vectensis*, a model species used in studies on metazoan development.

As mentioned above, *N. vectensis* has no true ovary and its sex cells develop in a gametogenic region of the mesentery [5], like other anthozoans [41, 42]. In sea anemones (Cnidaria, Anthozoa) "the term gonad is conditionally applied to the strips of tissue within the mesenteries where sexual products accumulate" [42, 43]. Describing of the local germ cells groups within gametogenic region of the mesentery, authors used different terms. So, Wilcox [34] called such structures in *N. vectensis* as "cysts" while Eckelbarger and Larson [44, 45] used the term "islands" in *Aurelia aurita*. We used the term "germ-cells groups". In these groups oocytes develop asynchronously, as is typical for many species of sea anemones [43], including *N. vectensis* [5, 34]. The maturation of large, polarized, vitellogenic oocytes begins with the germinal vesicle transformation to the karyosphere. The karyosphere, a specific structure that consists of composite multiple complexes of nuclear and cytoplasmic proteins [46, 47], protects the oocyte's genetic apparatus and decreases or completely stops its synthetic activity during the maturation process [48]. The formation of karyosphere during maturation is documented in different species of invertebrates and vertebrates [40–56]. In some animals, a decrease of the chromosomal transcriptional activity can be observed during the formation of the karyosphere and a complete cessation has been seen in the ring-shaped karyosphere. This was documented in insects [47, 48] as in the humans' preovulatory oocytes [51]. The morphological structure of the *N. vectensis* karyosphere is very similar to the karyosphere found in the insect *Tenebrio molitor* [48].

Based on the morphological features of the karyosphere in *N. vectensis* it is further assumed that chromosomes' synthetic activities die away near the end of the maturation process. This assumption is indirectly confirmed by the almost complete absence of visual contacts between the maturing oocytes and gastrodermal cell, where empty spaces are seen between them (Fig 5A and 5C compare with Fig 4A–4C).

The mature oligolecithal *Nematostella* egg contains a small amount of yolk that is evenly distributed throughout the ooplasm (isolecithal type, following [57]). In the present study, the dimension of eggs inside the egg masses varied between 158μ and 175μ., while Wilcox [34], Frizenwanker et al. [32] and Lee et al. [35] observed larger eggs (170μ–200μ; 210μ–270μ; 198μ–247μ, respectively). It is, however, well documented that cell sizes tend to decrease in the course of histological processing [38, 39]. Fertilization occurs at chromosomal status metaphase-II, outside the female body. The ejection of the first polar body, the fertilization and the segregation of the ooplasm occur almost simultaneously, as evidenced from the location of the

male pronucleus (either inside the egg or on its surface) and the noticeable yolk segregation (Fig 5C, 5E and 5G). Wilcox [34] and Fritzenwanker et al. [32] failed to observe the polar bodies and were unable to document *N. vectensis*' meiotic chromosome status at fertilization. Finding no polar bodies, Wilcox [34] suggested that the meiosis is completed in the female body, as is true for other cnidarians, ctenophores and sea urchins [45, 58–61] as well as for two anthozoan species [62]. Lee and co-authors [35], however, anectodicaly documented (an outcome that was not illustrated) in *N. vectensis* the release of two polar bodies from the animal pole into the jelly coat, suggesting that the polar bodies are displaced after the expansion of the eggs' jelly. This is also supported by the notion of Hand and Uhlinger [27] that the jelly coat in *N. vectensis* is preserved until the release of planulae from it, and Noda and Kanai [63] observation that the polar body in the hydrozoan *Pelmatohydra robusta* is found inside a "mucous-like substance". In contrast, we documented that in *N. vectensis* the polar bodies are shed into the space formed between the external edge of the oolemma and the inner edge of the jelly coat (Fig 6B–6D and 6K).

The most important event occurring during the fertilization process is the cortical reaction, during which the perivitelline space, which separates the egg's vitelline membrane from the ooplasm, is formed. This is a mechanism that protects the egg from being penetrated by multiple sperm (polyspermy). The basis of the cortical reaction is the hydration of the polysaccharides contained in the cortical granules [64, 65]. In *N. vectensis* the cortical layer of the egg is highly loaded with mucopolysaccharides, which start to develop at the onset of vitellogenesis and expand during the growth of the oocyte. By the end of vitellogenesis and during the oocytes' maturation, the entire surface of the outer cortex of the oocyte becomes rough. After fertilization the cortical layer is preserved, as is typical for many species of sea anemones [42]. In *N. vectensis* it hardens and becomes smooth (Fig 6L), except in the area of the animal pole, where the cortical granules are inserted into the space between the outer cortex's edge and the internal edge of the jelly coat (Fig 6J and 6K). While in *N. vectensis* we did not observe the typical cortical reaction accompanied by the formation of the large perivitelline space and the fertilization envelope, we did observed the formation of space between the superficial edge of egg's surface and the internal edge of the jelly coat at the site of sperm's penetration. The polar body was ejected exactly into this area (Fig 6B–6D and 6K). Thus, it can be assumed that based on the animal pole's limited space, this space is similar to the perivitelline space that exists in the fertilized eggs of other animals. Similarly, Clark and Dewel [62] described the cortical reaction in the anthozoan *Bunodosoma cavernanta* as occurring only at the animal pole. Obviously, eggs in *N. vectensis* might have a similar mechanism meant to prevent the penetration of more than one sperm into the area where the female pronucleus is located. While several spermatozoa can penetrate in *N. vectensis* into an egg simultaneously (physiological polyspermy) (Fig 6l), it is assumed that there is no mechanism to prevent polyspermy in any part of the yolk membrane except for the animal pole, similarly to documentations in other cnidarian species [63, 66, 67] and in siphonophores [68].

Here, we observed 2–4 spermatozoa heads inside *N. vectensis* fertilized eggs, while authors of [35] observed numerous spermatozoa on the egg surfaces at the pronucleus site in naïve eggs and single spermatozoa in other areas of the egg surfaces. Such a phenomenon is usually followed by the lysis of the excess sperm heads [64, 69]. As embryogenesis was not studied here no further information is available.

As mentioned earlier, the developing oocytes are surrounded by two types of gastrodermal cells: vacuolated glandular cells and trophocytes; the latter play an important role in the nutrition of oocytes during their growth [5]. The gastrodermal glandular cells accompany germ cells at all stages of oogenesis and probably they form the substances of the jelly coat when the oocytes ovulate into the gastric cavity. This is evidenced by similar tinctorial properties of the

glandular cells and the jelly coat (Figs 4B, 6B and 6G). Levitan et al. [9] using in situ hybridization method shown that the mesenterial glandular cells synthesize mucin 5B, which is the mains component of the jelly coat. We have established that the gastrodermal glandular cells produce different polysaccharides, including those resistant to amylase treatment. Similar results were obtained for several species of sea urchin [70, 71] where the extracellular jelly coats consist of neutral and acid mucopolysaccharide-protein complexes. The neutral muco-polysaccharides are amylase-resistant, but the functions of the sulfated polysaccharides of the jelly coat, as their biosynthesis, remain unknown. However, it is believed that they are responsible for inducing the species-specific acrosome reaction necessary for binding the sperm and fusing with the egg [72,73].

Immediately after spawning no oocytes with karyosphere were documented, though numerous previtellogenic and vitellogenic oocytes were seen within the gonadal region. These developing oocytes are probably the source of the next generations of shed eggs, an asynchro-nous type of germ cell development. Similarly, an asynchronous development of germ cells has been noted in the hydrozoan *Clytia hemisphaerica*, which can spawn daily in the laboratory [74]. Since there are no oocytes with karyosphere in the gonadal region of *N. vectensis* immedi-ately after spawning, we can assume that these oocytes have not completed their growth, did not reach a definitive size and could not begin the maturation process. In fish and amphibians only oocytes of definitive sizes acquire competence to begin maturation while responding to environmental and hormonal stimuli. It would be further interesting to study the effects karyo-spheres impose on the synthesis and accumulation of nutrients in *N. vectensis* oocytes through-out the maturation period, and it would be interesting to identify the mechanisms that initiate the maturation process and regulate the sex cells' competence to respond to the environmental factors. It would also be interesting to determine the potential fecundity of *N. vectensis* and the source of its recruited germ cells for use in the extended breeding season under laboratory conditions.

Acknowledgments

Author Contributions

Conceptualization: Elizabeth Moiseeva.

Data curation: Elizabeth Moiseeva, Guy Paz.

Funding acquisition: Baruch Rinkevich.

Methodology: Claudette Rabinowitz.

Supervision: Baruch Rinkevich.

Writing – original draft: Elizabeth Moiseeva.

Writing – review & editing: Elizabeth Moiseeva, Claudette Rabinowitz, Guy Paz, Baruch Rinkevich.

References

1. Williams RB. A redescription of the brackish water sea-anemone *Nematostella vectensis* Stephenson, with an appraisal of co-generic species. J Nat Hist 1975; 9: 51–64.

2. Hand C, Uhlinger KR. The unique, widely distributed estuarine sea anemone, *Nematostella vectensis* Stephenson: a review new facts, and questions. Estuaries 1994; 17: 501–508.

3. Daly M. A systematic revision of Edvardsiidae (Cnidaria, Anthozoa). Invert Biol 2002; 121: 212–225.

4. Sullivan JC, Ryan JF, Watson JA, Webb J, Mullikin JC, Rokhsar D, et al. Stellabase: the *Nematostella vectensis* genomics database. Nucleic Acids Res 2006; 34: D495–499. https://doi.org/10.1093/nar/gkj020 PMID: 16381919

5. Eckelbarger KJ, Hand C, Uhlinger KR. Ultrastructural features of the trophonema and oogenesis in the starlet sea anemone, *Nematostella vectensis* (Edvardsiidae). Invert Biol 2008; 127: 381–395.

6. Genikhovich G, Technau U. The starlet sea anemone Nematostella vectensis: an anthozoan model organism for studies in comparative genomic and functional evolutionary developmental biology. Cold Spring Harbor Protoc 2009a; pdb emo129.

7. Darling JA, Reitzel AR, Burton PM, Mazza ME Ryan YF, Sullivan JC et al. Rising starlet: the starlet sea anemone, *Nematostella vectensis*. BioAssays 2005; 27: 211–221.

8. Putnam NH, Srivastava M, Hellsten U, Dirks B, Chapman J, Salamov A, et al. Sea anemone genome reveals ancestral eumetazoan gene repertoire and genomic organization. Science 2007; 317: 86–94. https://doi.org/10.1126/science.1139158 PMID: 17615350

9. Levitan S, Sher N, Brekhman V, Ziv T, Labzens E, Lotan T. The making of an embryo in a basal metazoan: Proteomic analysis in the sea anemone *Nematostella vectensis*. Ptoteomics 2015; 15: 4096–4104.

10. Harter VL, Matthews RA. Acute and chronic toxicity test methods for *Nematostella vectensis* Stephenson. Bull Environ Contam Toxicol 2005; 74: 830–836. PMID: 16097314

11. Goldstone JV. Environmental sensing and response genes in cnidarian: the chemical defensome in the sea anemone *Nematostella vectensis*. Cell Biol Toxicol 2008; 24: 483–502. https://doi.org/10.1007/s10565-008-9107-5 PMID: 18956243

12. Fraune S, Forêt S, Reitzel AM. Using *Nematostella vectensis* to study the interactions between genome, epigenom, and bactetia in a changing environment. *Frontiers in Marine*. Science 2016; 3:148. https://doi.org/.3389/fmars/2016/00148.

13. Finnerty JR, Pang K, Burton P, Paulson D, Martindale MQ. Origins of bilateral symmetry: *Hox* and *dpp* expression in a sea anemone. Science 2004; 304: 1335–1337. https://doi.org/10.1126/science.1091946 PMID: 15131263

14. Finnerty JR, Martindale MQ. Ancient origin of axial patterning genes: *Hox* genes and *ParaHox* genes in the Cnidaria. Evol Dev 1999; 1:16–23. PMID: 11324016

15. Scholz CB, Technau U. The ancestral role of Brachyury: expression of NemBra I in the basal cnidarian *Nematostella vectensis* (Anthozoa). Dev Genes Evol 2003; 212: 563–570. PMID: 12536320

16. Martindale MQ, Pang K, Finnerty JF. Investigating the origins of triploblasty: "mesodermal" gene expression in a diploblastic animal, the sea anemone *Nematostella vectensis* (phylum, Cnidaria; class, Anthozoa). Development 2004; 131: 2463–2474. https://doi.org/10.1242/dev.01119 PMID: 15128674

17. Frizenwanker GH, Saina M, Technau U. Analisys of forkhead and snail expression reveals epithelial-mesenchymal transitions during embryonic and larval development of *Nematostella vectensis*. Dev Biol 2004; 275: 389–402. https://doi.org/10.1016/j.ydbio.2004.08.014 PMID: 15501226

18. Primus A, Freeman G. The cnidarian and the canon: the role of *Wnt* /beta-catening signaling in the evolution of methazoan embryos. Bioassay 2004 26: 474–478.

19. Kumburegama S, Wijesena N, Wikramanayake AH. Detecting expression patterns of *Wnt* pathway components in *Nematostella vectensis* embryos. Methods Mol Biol 2008; 469: 55–67. https://doi.org/10.1007/978-1-60327-469-2_6 PMID: 19109703

20. Matus DQ, Magie CR, Pang K, Martindale MQ, Thomsen GH. The *Hendgehog* gene family of the cnidarian, *Nematostella vectensis*, and implications for understanding metazoan *Hendgehog* pathway evolution. Dev Biol 2008; 313: 501–518. https://doi.org/10.1016/j.ydbio.2007.09.032 PMID: 18068698

21. Reitzel AM, Burton PM, Krone C, Finnerty JR. Multiple developmental trajectories of the starlet sea anemone *Nematostella vectensis* (Stephenson): Sexual reproduction, asexual fission, and regeneration. Invert Biol 2007; 126: 99–112.

22. Burton PM, Finnerty JR. Conserved and novel gene expression between regeneration and asexual fission in *Nematostella vectensis*. Dev Genes Evol 2009; 219: 79–87. https://doi.org/10.1007/s00427-009-0271-2 PMID: 19184098

23. Layden MJ, Rentzsch F, Röttinger E. The rise of the starlet sea anemone *Nematostella vectensis* as a model system to investigate development and regeneration. Wiley Interdisciplinary Reviews: Developmental Biology 2016; 5:408–428. https://doi.org/10.1002/wdev.222 PMID: 26894563

24. Watanabe H, Hoang VT, Mättner R, Holstein TW. Immortality and the base of multicellular life: lessons from cnidarian stem cells. Sem. Cell Dev Biol 2009; 20: 1114–1125.

25. Marlow HQ, Srivastava M, Matus DQ, Rokhsar D, Martindale MQ. Anatomy and development of the nervous system of *Nematostella vectensis*, an Anthozoa Cnidarian. Dev Neurobiology 2009; 69: 235–254.

26. Saina M, Genikhovich G, Renfer E, Technau U. BMPs and chordin regulate patterning of the directive axis in a sea anemone. Proc Natl Acad Sci USA 2009; 106: 18592–18597. https://doi.org/10.1073/pnas.0900151106 PMID: 19833871

27. Hand C, Uhlinger KR. The culture, sexual and asexual reproduction, and growth of the sea anemone *Nematostella vectensis*. Biol Bull 1992; 182: 169–176.

28. Fritzenwanker JH, Technau U. Induction of gametogenesis in the basal cnidarian *Nematostella vectensis* (Anthozoa). Dev Genes Evol 2002; 212: 93–103.

29. Genikhovich G, Technau U. Induction of spawning of the starlet anemone Nematostella vectensis, in vitro fertilization of gametes, and dejellying zygotes. Cold Spring Harbor Protoc 2009b; pdb. Prot 5282.

30. Extavour CG, Pang K, Matus DQ, Martindale MQ. *Vasa* and *nanos* expression patterns in a sea anemone and the evolution of bilaterian germ cell specification mechanisms. Evol Dev 2005; 7: 201–215. https://doi.org/10.1111/j.1525-142X.2005.05023.x PMID: 15876193

31. Frank PG, Bleakney JS. Histology and sexual reproduction of the anemone *Nematostella vectensis* Stephenson 1935. J Nat Hist 1976; 10: 441–449.

32. Fritzenwanker JH, Genikhovich G, Kraus Y, Technau U. Early development and axis specification in the sea anemone *Nematostella vectensis*. Dev Biol 2007; 310: 264–279. https://doi.org/10.1016/j.ydbio.2007.07.029 PMID: 17716644

33. Uhlinger KR. Sexual reproduction and early development in the estuarine sea anemone, Nematostella vectensis Stephenson 1935. PhD. Thesis. The University of California- Davis, 1997.

34. Wilcox JA. Oocyte meiotic state, developmental plasticity, and independence of cytokinesis from karyokinesis during early development in the cnidarian Nematostella vectensis. PhD. Thesis. The University of Florida, 2001.

35. Lee PN, Kumburegama S, Marlow HQ, Martindale MQ, Wikramanayake AH. Asymmetric developmental potential along animal-vegetal axis in the amthozoan cnidarian, *Nematostella vectensis*, is mediated by Dishevelled. Dev Biol 2007; 310: 169–186. https://doi.org/10.1016/j.ydbio.2007.05.040 PMID: 17716645

36. Stefanik DJ, Friedman LE, Finnerty JR. Collecting, rearing, spawning and inducing regeneration of the starlet sea anemone, *Nematostella vectensis*. Nature Protocols 2013; 8: 916–923. https://doi.org/10.1038/nprot.2013.044 PMID: 23579780

37. Rabinowitz C, Moiseeva E, Rinkevich B. *In vitro* cultures of ectodermal monolayers from the model sea anemone *Nematostella vectensis*. Cell and Tissue Research 2016; 366: 693–705. https://doi.org/10.1007/s00441-016-2495-6 PMID: 27623804

38. Lillie RD. Histopathological technic and practical histochemistry. 2nd ed. New York: McGraw-Hill, 1954.

39. Pearse AG. Histochemistry: Theoretical and Applied. 2-nd edition. London: Churchill A, and J, 1960.

40. Tucker RP, Shibata B, Blankenship TN. Ultrastructure of the mesoglea of the sea anemone *Nematostella vectensis* (Edvardsiidae). Invertebrate Biol 2011; 130: 11–24.

41. Belousoff LV. The dinamics architecture of a developing organism. Dordrecht: Kluwer Academic, Netherlands, 1998.

42. Bocharova E. Reproduction of sea anemones and other hexacorals. In: Goffredo S, Dubinsky Z, editors. The Cnidaria, Past, Present and Future. The world of meduse and her sisters. Part IV. The Switzerland: Springer, 2016: pp.239–248.

43. Bocharova ES, Kozevich IA. Modes of reproduction in sea anemones (Cnidaria, Anthozoa). Biol Bull 2011; 38: 1283–1295.

44. Eckelbarger KJ, Larson RL. Ovarian morphology and oogenesis in *Aurelia aurita* (Scyphozoa: Semaeostomeae): ultrastructural evidence of heterosynthetic yolk formation in a primitive metazoan. 1988. Mar Biol; 100:103–115.

45. Chatlynne LG. A histochemical study of oogenesis in the sea urchin, *Strongylocentrotus purpuratus*. Biol Bull 1969; 136: 167–184. https://doi.org/10.2307/1539811 PMID: 5794095

46. Gruzova MN. The nucleus during oogenesis with special reference to extrachromosomal structures. In: Detlaf TA, Vassetsky SG, editors. Oocyte growth and maturation. New York, London: Plenum Press; 1988. pp.77–163.

47. Gruzova MN, Parfenov VN. Karyosphere in oogenesis and intranuclear morphogenesis. Int Rev Cytol 1993; 144: 1–52. PMID: 7686538

48. Bogolyubov D, Parfevov V. Immunogold localization of RNA polymerase II and pre-mRNA splicing factors in *Tenebrio molitor* oocyte nuclei with special emphasis on karyosphere development. Tissue and Cell 2001; 33: 549–561. https://doi.org/10.1054/tice.2001.0210 PMID: 11827099

49. Gruzova MN. Karyosphere in oogenesis. Tsitologiia 1976; 17: 219–37. (in Russian, English abstract).

50. Gruzova MN, Parfenov VN. Ultrastructure of late oocyte nuclei in *Rana temporaria*. J Cell science 1977; 28: 1–13. PMID: 304451

51. Parfenov V, Pochukalina G, Dudina L, Kostyuchek D, Grusova M. Human antral follicle: oocyte nucleus and karyosphere formation (electron microscopic and autoradiographic data). Gamete Res 1989; 22: 219–231. https://doi.org/10.1002/mrd.1120220209 PMID: 2468591

52. Kubrakiewicz J, Bilìnski SM. Extrachromosomal amplification of rDNA in oocytes of *Hemerobius spp*. (Insecta, Neuroptera). Chromosoma 1995; 103: 606–612. PMID: 7587583

53. Gall JG, Tsvetkov A, Wu Z, Murphy C. Is the sphere organelle /coiled body a universal nuclear component? Dev Genet 1995; 16: 25–35. https://doi.org/10.1002/dvg.1020160107 PMID: 7758244

54. Bogolyubov D, Alexandrova O, Tzvetkov A, Parfenov V. An immunoelectron study of karyosphere and nuclear bodies in oocytes of mealworm beetle, *Tenebrio molitor* (Coleoptera: Polyphaga). Chromosoma 2000; 109: 415–425. PMID: 11072797

55. Batalova FM, Bogolyubov DS, Parfenov VN. Interchromatin granule clusters of the Scorpionfly oocytes contain poly (A) + RNA, heterogeneous ribonucleoproteins A\B and mRNA export factor NXF 1. Cell Biol Int 2010; 34: 1163–1170. https://doi.org/10.1042/CBI20090434 PMID: 20658966

56. Pochukalina GN, Stepanova IS. Interchromatin granules clusters of mouse preovulatory oocytes are enriched with some components of mRNA export machinery. Ann Res Rev Biol 2014; 4: 79–92.

57. Beloussov LV. The problem of biological morphogenesis: General approach and mechano-geometrical models. In: Kull K, Tiivel T, editors. Lectures in Theoretical Biology. Valgus, Tallin, Estonia; 1988. pp. 55–64.

58. Masui Y. Meiotic arrest in animal oocytes. In: Metz C, Monroy A, editors. Biology of fertilization. vol.1, Florida: Academic Press; 1985. pp. 189–219.

59. Gilbert SF. Developmental Biology. 4th ed. Sinauer: Sunberland, 2000.

60. Fautin DG. Reproduction in Cnidaria. Can J Zool 2002; 80: 1735–1754.

61. Byrum CA, Martindale MQ. Gastrulation in the Cnidaria and Ctenophora. In: Stern CD, editor. Gastrulation: From Cells to Embryos. New York, Cold Spring Harbor: Cold Spring Harbor Laboratory Press; 2004. pp.33–50.

62. Clark WM, Dewel WC. The structure of gonads, gametogenesis, and sperm-egg interaction in the Anthozoa. Amer Zool 1974; 14: 495–510.

63. Noda K, Kanai C. Light and electron microscopic studies on fertilization of *Pelmatohydra robusta*. 1. Sperm entry to specialized region of the egg. Dev Growth Different 1981; 23: 401–413.

64. Ginsburg AS. Phylogenetic changes in the type of fertilization. In: Mli'kovsky J, Novác VJA, editors. Evolution and Morphogenesis. Prague: Academia 1985, pp.459–466.

65. Abbineni PS, Hilbert JE, Coorssen JR. Critical role of cortical vesicles in dissecting regulated exocytosis: Overview of insights into fundamental molecular mechanisms. Biol Bull 2013; 224: 200–217. https://doi.org/10.1086/BBLv224n3p200 PMID: 23995744

66. Freeman G. The role of polarity in the development of the hydrozoan planula larva. Wilhelm Roux's Arch Dev Biol 1981; 190: 168–184.

67. Freeman G, Miller RL. Hydrozoan eggs can only be fertilized at the site of polar body formation. Dev Biol 1982; 94: 142–152. PMID: 7152101

68. Carrè D, Sardet C. Sperm chemotaxis in siphonophores. Biol. Cell 1981; 40: 119–128.

69. Ginsburg AS. Fertilization in fishes and the problem polyspermy. Detlaf TA, editor. Washington: National Marine Fisheries Service, NOAA, U.S. Department of Commerce and the National Science Foundation, Washington, D.C; 1972.

70. Jondeung A, Czihak G. Histochemical studies of jelly coat of sea-urchin eggs during oogenesis. Histochemistry; 1982; 76: 123–136. PMID: 6217173

71. Abe H, Kinoh H, Oikawa T, Suzuki N. The egg-jelly macromolecule, a fucose sulphate glycoconjugate, originates from the accessory cells of the ovary in the sea urchin *Hemicentrotus pulcherrimus*. Roux's Arch Dev Biol 1992; 201: 179–189.

72. Vilela-Silva AC, Castro MO, Valente AP, Biermann CH, Mourao PA. Sulfated fucans from the egg jellies of the closely related sea urchins *Spongylocentrotus droebachiensis* and *Strongylocentrus pallidus* ensure species-specific fertilization. J Biol Chem 2002; 277: 379–387. https://doi.org/10.1074/jbc.M108496200 PMID: 11687579

73. Cinelli LP, Andrade L, Valente AP Mouräo PA. Sulfated α-L-galactans from the sea urchin ovary: Selective 6-desulfation as eggs are spawned. Glycobiology 2010; 20:702–709. https://doi.org/10.1093/glycob/cwq017 PMID: 20147451

74. Amiel A, Chang P, Momose T, Houliston E. *Clytia hemispharetica*: a cnidarian model for studying oogenesis. In: Verlhac M-H, Villeneuve A, (editors). Oogenesis: the universal process, Wiley: 2010, p.81–101.